Efficient Transient Simulation of High-Speed Interconnects Characterized by Sampled Data

Wendemagegnehu T. Beyene, *Member, IEEE,* and José E. Schutt-Ainé, *Member, IEEE*

***Abstract*—In this paper, we present an algorithm for efficient simulation of high-speed interconnects characterized by sampled data. The method constructs pole-zero models of arbitrary interconnects using robust rational approximations of the measured or simulated scattering parameters. In order to obtain accurate interpolations of the data over a wide frequency range, a set of powerful techniques is applied to deal with the resulting ill-conditioned Vandermonde-like approximation matrices. By utilizing the analytic properties of the scattering parameters, the algorithm efficiently generates multiport pole-residue models. The models are combined with the lumped/distributed components for direct time- or frequency-domain simulations. The method can easily be implemented into conventional simulators such as simulation program with integrated circuit emphasis (SPICE) and advanced statistical analysis program (ASTAP) or reduced-order modeling techniques such as asymptotic waveform evaluation (AWE), complex frequency hopping (CFH), and Padd approximation via Lancros Process (PVL) for transient simulation of high-speed interconnect networks. Examples of linear and nonlinear networks are given to demonstrate the validity and accuracy of the method.**

***Index Terms*— High-speed interconnect, rational approximation, scattering parameter.**

I. Introduction

As WIRING density in high-performance packaging increases, the interconnect geometry becomes nonuniform and the cross-sectional dimensions become smaller. Consequently, the interconnect and dielectric losses, dispersions, and discontinuities have to be considered in the analysis of an electronic package. These frequency-dependent phenomena of interconnects are most accurately characterized by measured or simulated data than by closed-form functionals [1]. For example, the skin effect of an interconnect is best characterized by frequency-domain data. The transient analyses of systems described in tabular forms cannot efficiently be performed using conventional simulators such as simulation program with integrated circuit emphasis (SPICE) [2] and advanced statistical analysis program (ASTAP) [3], or using methods based on Padé syntheses such as asymptotic waveform evaluation (AWE) [4]–[6], complex frequency hopping (CFH) [6], [7], and Padd approximation via Lancros process (PVL) [8], [9].

The incorporation of interconnects characterized by frequency-domain data obtained from measurements or full-wave electromagnetic solvers into circuit simulators are complex and computationally intensive. Since nearly all interconnects are driven or terminated by nonlinear devices, the method must combine the time-domain and frequency-domain descriptions [10], [11]. The most straightforward approach is to calculate the impulse response of the measured network using the inverse fast Fourier transform (IFFT) and to apply the discrete time solution to solve the whole system for a given input waveform [12]. Such an approach requires that at every simulation time step, the impulse response be convoluted with the entire computed input waveform. The IFFT used to transform frequency-domain data into time-domain data requires special attention to avoid aliasing. Extrapolation and low-pass filtering of the frequency-domain data are required to reduce the time-domain ripple associated with taking the IFFT. A very large number of samples is required for an adequate representation of the impulse functions, which increases the convolution computation time of the transient response. Although this method gives a reliable solution, it is not fast enough to provide results of a large system in an acceptable time interval.

A more efficient method of incorporating measured data into circuit simulators can be obtained by first partitioning the global network into subnetworks characterized either by component-based model or sampled data. Then, pole-residue representation of each component-based model subnetwork is found via the Padé approximation. For the measured subnetwork, rational function approximation is used to drive the models. Then the pole-residue level representations of component-based and measured subnetworks are combined to form the global network. The pole-residue models are incorporated as submatrices into the system matrix of the global network using recursive convolution, and then the entire system including the nonlinear devices is solved in the time domain. Thus, the size of the overall circuit to be simulated is reduced. The method does not require a numerical transform treatment or the smoothing and band-limiting filtering of a large number of points, which are often required in conventional methods.

In Section II, an overview of reduced-order modeling techniques is given. In Section III, the scattering parameter formulation of a multiport network is presented. In Section IV, the rational approximation is discussed and the numerical prop-

Manuscript received December 27, 1996; revised September 3, 1997. This paper was supported by AFOSR via the MURI Program under Contract F49620-91-0025 and by the National Science Foundation under Grant NSF EEC 89-43166.

W. T. Beyene is with Hewlett-Packard Company, Westlake Village, CA 91362 USA (e-mail: wbeyene@wlv.hp.com).

J. E. Schutt-Ainé is with the Department of Electrical and Computer Engineering, University of Illinois, Urbana, IL 61801 USA (e-mail: jose@decwa.ece.uiuc.edu).

Publisher Item Identifier S 1070-9894(98)00594-5.

erties of the approximation method are given. In Section V, the time-domain macromodels are generated from pole-residue representations using recursive convolution. Numerical results are shown in Section VI. Finally, the conclusion is given in Section VII.

II. Order-Reduction Techniques

Recently, model-order reduction techniques such as AWE, CFH and PVL have been used for the analyzes of large linear lumped and distributed networks. The methods employ Padé synthesis to obtain reduced-order rational approximations of high-order transfer functions. As a result, the complexity of the analyzes of the systems are simplified [4]–[9]. Typical efficiency gains of two to three orders of magnitude speedup over those for traditional simulation techniques have been obtained with AWE [4]–[6]. However, AWE, CFH, and PVL are not quite suitable for networks characterized by tabular data, as the derivatives at selected expansions cannot accurately be calculated to find the moments. In [13], a hybrid technique is used by first approximating the function by rational functions over partitioned frequency ranges, and then using the derivative of the rational functions to obtain the moments. The moments, however, obtained using this method are order dependent violating the definition of the Taylor series.

Several methods have been suggested to increase the versatility of AWE and CFH methods. In [14]–[15], a methodology for incorporating subnetworks characterized by measured data is presented. The component-based subnetwork is reduced and the measured subnetworks are incorporated as submatrices in the modified nodal admittance analysis (MNA) matrix [16], the formulation employed by conventional simulators, of the global circuit to be solved at a set of frequency points. Then, IFFT is performed on the data points to obtain the response in the time domain.

III. Multiport Network

A general network, N, can be partitioned into a number of subnetworks, N_i, $\{i = 1, \cdots, N\}$ as shown in Fig. 1. The analysis of the global network, N, can be carried out by generating a pole-residue model for each subnetwork. Then, each subnetwork can be represented as a multiport network that can be characterized in terms of one of the following parameters, namely, admittance, impedance, hybrid, or transmission parameters. The Padé synthesis is often used to compute the low-order approximation of the admittance matrix for the subnetworks characterized by a lumped or distributed

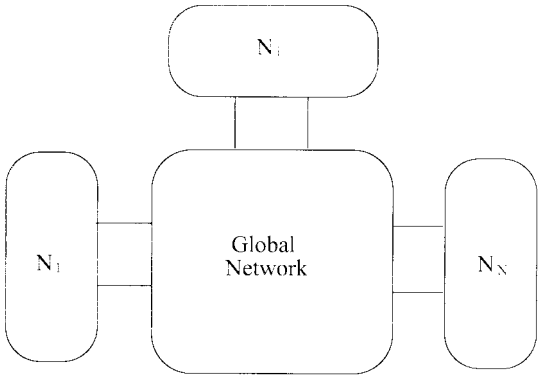

Fig. 1. Partitioned multiport subnetworks, $N_i, \{i = 1, ..., N\}$, are component-based or measured subnetworks.

model. The measured subnetwork is often characterized by frequency-domain data using the scattering matrix.

Although either the characteristic impedance or the characteristic admittance can be used to describe the measured subnetwork, they are difficult to derive, approximate or measure accurately for arbitrary interconnects. However, scattering parameters, in addition to their unique meanings, are stable parameters readily available from full-wave electromagnetic analyzes or measurements. Scattering parameters of complex structures can be measured with high accuracy using one of the commercially available network analyzers. Scattering parameters can also be derived from *TEM, quasi-TEM* or frequency-dependent $R,\ L,\ C$ and G parameters.

An n-port network can be characterized by $2n \times 2n$ scattering matrix. The frequency-domain scattering matrix relates the incident-wave and the reflected-wave vectors as

$$\begin{aligned} B_1 &= S_{11}A_1 + S_{12}A_2 \\ B_2 &= S_{21}A_1 + S_{22}A_2 \end{aligned} \tag{1}$$

where S_{ij}'s are the $n \times n$ scattering submatrices describing the measured network, A_i's and B_i's are the frequency-domain forward and backward waves, respectively. Rational approximation is, then, used to obtain the reduced-order model of the scattering parameters of the measured subnetworks. Once the pole-residue pairs are determined from the above equations, each subnetwork is treated as a multiterminal device in the MNA matrix of the global network. The direct integration of the scattering matrix into a circuit simulator is described in [17]. The stamp of the MNA matrix corresponding to the measured n-port subnetwork is (2), as shown at the bottom of the next page, where Z_i, R_i, and I are the $n \times n$ reference impedance, the real part of the reference impedance, and

$$\begin{bmatrix} & & & & I & \\ & & & & -I & \\ & & & & & I \\ & & & & & -I \\ (I-S_{11}) & -(I-S_{11}) & -S_{12}R_1^{\frac{1}{2}}R_2^{-\frac{1}{2}} & S_{12}R_1^{\frac{1}{2}}R_2^{-\frac{1}{2}} & -(S_{11}Z_1+Z_1^*) & -S_{12}Z_2R_1^{\frac{1}{2}}R_2^{-\frac{1}{2}} \\ -S_{21}R_2^{\frac{1}{2}}R_1^{-\frac{1}{2}} & S_{21}R_2^{\frac{1}{2}}R_1^{-\frac{1}{2}} & (I-S_{22}) & -(I-S_{22}) & -S_{21}Z_1R_2^{\frac{1}{2}}R_1^{-\frac{1}{2}} & -(S_{22}Z_2+Z_2^*) \end{bmatrix} \begin{bmatrix} V_1^+ \\ V_1^- \\ V_2^+ \\ V_2^- \\ I_1 \\ I_2 \end{bmatrix} = \begin{bmatrix} \\ \\ \\ \\ 0 \\ 0 \end{bmatrix} \tag{2}$$

the identity submatrices respectively. The pairs (V_1, V_2) and (I_1, I_2) are terminal voltages and currents, respectively.

The global matrix to be solved is smaller; consequently, the stability and the speed of the analysis of the global network are improved because the large problem is converted to smaller problems. Since IFFT is avoided, arbitrary components can be simulated in the time domain. Using the integration formula in (2), the pole-residue pairs can be integrated in SPICE-like simulators with the remaining linear and nonlinear networks. In the following section, we will describe the method of approximating the scattering parameters by a rational function over a wide frequency range using frequency normalization and shifting, and Householder *QR* orthogonalization to solve the resulting system of equations.

IV. Approximation

Polynomials are the simplest and most common means of approximating functions. Although the existence and uniqueness of polynomial interpolations of arbitrary data can be proved using the Weierstrass approximation theorem, polynomial functions are not used to approximate transfer functions of networks. Polynomials are not suitable to represent frequency responses of electrical networks, because polynomials do not work well in approximating the behavior of functions near their poles. In contrast, rational functions do capture the behavior of networks around the poles and their partial fraction expansions can readily be used to obtain the time-domain responses as sums of trigonometric and/or exponential functions. Hence, the transfer functions of electrical networks can be approximated by the least maximum error by rational functions rather than that by polynomial functions of comparable order.

The idea of approximating arbitrary functions using rational functions is quite an old problem [18]–[20]. The recent developments of lossy transmission line simulation techniques using transfer functions have regenerated considerable interest in accurate and efficient methods to determine the poles and zeros (residues) directly from the time-domain or frequency-domain responses [21], [22]. Rational interpolation, in partial fraction expansion form, is one of the most suitable and accurate rational approximation methods of distributed systems. However, unlike polynomial approximation, rational approximation is not linear space. The approximation matrices are ill-conditioned and the calculation of the polynomial coefficients is numerically sensitive; consequently, the computational procedures are subject to problems of great numerical inaccuracy and are limited by the precision of the computer.

In [13], [22], and [23], partitioned or section-by-section approximation over a smaller domain is proposed to avoid the numerical ill-conditioning of the rational approximation. The frequency range is partitioned into sections and a low-order approximation is applied in each section. Once an approximation is obtained in a section, the value of the approximation function is subtracted from the corresponding data, and the resulting data are again fitted using the next section. The procedure is repeated until the data in the last frequency section are approximated. Then, the whole procedure starting from the first section is repeated until the approximation converges. Although this method constructs better conditioned matrices, the process can introduce some erroneous dynamics when subtracting the results of already computed approximations from the exact data. Consequently, the convergence of the method can be extremely slow when the method is applied to complex or periodic data . However, the method can be used to give a good fit with aperiodic data.

In [24], a rational interpolation algorithm is used for optimal transient simulation of transmission lines. The method is global in the sense that one rational approximation is used over the entire frequency range. The method is very efficient and gives good approximations for most practical problems. When higher-order approximations of complex systems are sought, however, the method has numerical inaccuracies due to the ill-conditioning of the matrices and the normal equation method the algorithm employs to obtain least-squares solutions. In this work, optimal conditioning and Householder *QR* orthogonal triangularization and automatic adjustment of order approximation are introduced to guarantee the existence of a stable rational approximation of a complex system over a wide approximation domain.

A. Interpolation by Rational Functions

A network function $H(s)$ of a linear system can be approximated by a rational function that interpolates the given function at given points. The rational function can be in a pole-residue, pole-zero form or as a ratio of polynomials. Suppose the network function, $F(s_i)$, given either analytically or at given points, s_i, is approximated by a rational function of degree (ξ, ϑ)

$$H_{\xi,\vartheta}(s) = \frac{Q_\xi(s_i)}{P_\vartheta(s_i)} = \frac{q_0 + q_1 s + q_2 s^2 + \cdots + q_\xi s^\xi}{1 + p_1 s + p_2 s^2 + \cdots + p_\vartheta s^\vartheta} \tag{3}$$

with p_0 normalized to unity. Equation (3) contains $n = \xi + \vartheta + 1$ free coefficients, hence, at most n independent parameters. The coefficients are determined so that the approximating function evaluated at the same frequency points gives close approximations to the function $F(s)$. For specified finite functional values $y_i = F(s_i)$, $\{i = 0, \cdots, k-1\}$ and k specified distinct points, s_i, the resulting equations give

$$\frac{Q_\xi(s_i)}{P_\vartheta(s_i)} - y_i = 0. \tag{4}$$

By canceling the denominators in (2), one obtains the linear homogenous system of k equations in n unknowns

$$Q_\xi(s_i) - y_i P_\vartheta(s_i) = 0 \tag{5}$$

which can be written in a matrix form as (6), as shown at the bottom of the next page.

The solution of the system is not guaranteed in general. The linear problem in (6) is not necessarily equivalent to the interpolation problem in (4). The rational function does not necessarily satisfy the interpolation conditions if the denominator polynomial has a zero for one of the given abscissas s_i. As a consequence, the numerator polynomial must also have the same zero, so both polynomials have a common linear factor $(s - s_i)$ that cancels. The resulting rational function

will generally no longer satisfy the interpolation condition for s_i, as $H(s_i) \neq y_i$. Hence, the interpolation problem has no solution for the prescribed degrees ξ and ϑ of the numerator and denominator polynomials, respectively. In this case, the order of approximation has to be adjusted to guarantee the existence of the solution.

To find the conditions under which a solution exists, it is important to point out that the columns of $\mathbf{V}$ form independent vectors; hence, $\mathbf{V}$ is full rank. The rank of the matrix $\mathbf{V} \in \mathbf{R}^{k\times n}$ given by (6) is equal to $\min(n,k)$. There are two possible situations:

1) $k \geq n$, and (6) is a full-rank overdetermined system;
2) $k < n$ and (6) is a full-rank underdetermined system.

The first case is an interpolation problem, and the case $k > n$ can be reduced to the case $k = n$ by writing (4) in an appropriate form. For the $k = n$ problem, (6) is consistent for any $Y \in \mathbf{R}^n$, and $X = \hat{\mathbf{V}}^{-1}Y$ is the unique solution, where $\hat{\mathbf{V}} \in \mathbf{R}^{n\times n}$ is reformulated $\mathbf{V}$. In the second case, $k < n$, there is, in general, an infinite number of solutions. The complete solution set s given by

$$X = V^T(VV^T)^{-1}Y + (I - V^T(VV^T)^{-1}V)b \qquad (7)$$

where b is arbitrary.

For higher-order approximations over a wider approximation range, the system in (6) is highly ill-conditioned and nearly singular because of the large difference between the maximum and minimum frequencies raised to the order of approximation. Even with proper frequency normalization, the computational procedures are limited by the numerical range and precision of the computer. The numerical considerations are discussed in detail in Section IV-C.

B. Approximation of a Network Function

The approximation algorithm can be made more efficient and accurate by utilizing the special properties of network functions. For instance, constraints necessary to insure a physically realizable passive network require that the transfer function be a rational fraction of polynomials in s. The coefficients of these polynomials must be real, and all roots of the denominator polynomial must have negative or zero real parts.

In addition, network functions are analytic functions of a complex variable; hence, their real and imaginary parts are related by Cauchy–Riemann equations. In an electrical network, some constraints remain between the frequency variations of resistance and of reactance, or conductance and sucepectance, just as in the Kramers–Kroning relations between real and imaginary parts of permittitvity. The locations of zeros and poles of a passive network are constrained to the left-half complex frequency plane due to the analytic character of the network function. Thus, the response of a passive network can only decay in time from any transient initial state. The consequence of this property is that only the real part, imaginary part, angle, or magnitude of the network function has to be approximated and the network function itself can be found from the resulting approximation.

Next, we will discuss the procedure for determining a network function as a rational function of s, using the real parts of the function. The real part of a network function (3) can be specified as the even part of $H(s)$ replacing $-s^2$ by ω^2. The real part of the original function is fitted with the real rational polynomial function of the squared variable

$$\mathrm{Re}(H_{\xi,\vartheta}(s)) = \frac{c_0 + c_1 s^2 + c_2 s^4 + \cdots + c_\xi s^{2\xi}}{1 + p_1 s^2 + p_2 s^4 + \cdots + p_\vartheta s^{2\vartheta}}. \qquad (8)$$

Since the poles of the even function of $F(s)$ are those of both $F(s)$ and $F(-s)$, those belonging to $F(s)$ lie in the left-half plane. Thus, the denominator coefficients of $H(s)$ in (3) can be obtained from (8). The following system of equations results from matching the real parts of the original function with (8) at the set of frequencies where the superscript "r" indicates the real part of a complex value (9), as shown at the bottom of the next page.

The conditions for the existence of the solution are as stated in Section IV-B. Factoring the denominator and taking only the left-half plane poles, the partial fraction expansion of the transfer function is constructed. Not a single unstable (positive) pole is obtained, since the polynomial roots are determined in terms of the square poles. The purely imaginary single poles on the imaginary axis are rejected as spurious since the rational function in (8) has double poles. Hence, the order of the approximating function must be set to a value greater than or equal to the actual order sought. The remaining negative poles are used to formulate the stable partial fraction expansion of

$$\underbrace{\begin{bmatrix} 1 & s_0 & s_0^2 & \cdots & s_0^\xi & -s_0y_0 & -s_0^2y_0 & \cdots & -s_0^\vartheta y_0 \\ 1 & s_1 & s_1^2 & \cdots & s_1^\xi & -s_1y_1 & -s_1^2y_1 & \cdots & -s_1^\vartheta y_1 \\ & \vdots & & & & & & & \\ 1 & s_{k-1} & s_{k-1}^2 & \cdots & s_{k-1}^\xi & -s_{k-1}y_{k-1} & -s_{k-1}^2y_{k-1} & \cdots & -s_{k-1}^\vartheta y_{k-1} \end{bmatrix}}_{\mathbf{V}} \underbrace{\begin{bmatrix} q_0 \\ q_1 \\ q_2 \\ \vdots \\ q_\xi \\ p_1 \\ p_2 \\ \vdots \\ p_\vartheta \end{bmatrix}}_{\mathbf{X}} = \underbrace{\begin{bmatrix} y_0 \\ y_1 \\ \vdots \\ y_{k-1} \end{bmatrix}}_{\mathbf{Y}} \qquad (6)$$

the transfer function as

$$H(s) = k_\infty + \sum_{i=1}^{\vartheta'} \frac{k_i}{s + p_i} \tag{10}$$

where p_r and k_r are complex poles and residues and k_∞ represents any direct coupling between the input and the output, and $\vartheta' \leq \vartheta$, and $\vartheta - \vartheta'$ is the number of rejected purely imaginary poles.

Solving for residues using only the stable poles gives a better approximation than the approach in [23] where the unstable poles with the associated residues are discarded at the final phase. No error is introduced in discarding the erroneous poles because the residues are calculated by matching the function using the remaining selected poles. Matching the real and imaginary parts of each element of the original matrix transfer function with the corresponding parts of the elements of (10) at the set of points leads to the following set of linear system of equations

$$\underbrace{\begin{bmatrix} 1 & \frac{-p_1}{\omega_0^2+p_1^2} & \cdots & \frac{-p_\vartheta}{\omega_0^2+p_\vartheta^2} \\ 1 & \frac{-p_1}{\omega_1^2+p_1^2} & & \frac{-p_\vartheta}{\omega_1^2+p_\vartheta^2} \\ \vdots & & & \\ 1 & \frac{-p_1}{\omega_{k-1}^2+p_1^2} & \cdots & \frac{-p_\vartheta}{\omega_{k-1}^2+p_\vartheta^2} \\ 0 & \frac{-\omega_0}{\omega_0^2+p_1^2} & & \frac{-\omega_0}{\omega_0^2+p_\vartheta^2} \\ \vdots & & & \vdots \\ 0 & \frac{-\omega_{k-1}}{\omega_{k-1}^2+p_1^2} & \cdots & \frac{-\omega_{k-1}}{\omega_{k-1}^2+p_\vartheta^2} \end{bmatrix}}_{\mathbf{M}} \underbrace{\begin{bmatrix} k_\infty \\ k_1 \\ \\ k_\vartheta \end{bmatrix}}_{\mathbf{K}} = \underbrace{\begin{bmatrix} y_0^r \\ y_1 \\ \vdots \\ y_{k-1}^r \\ y_1^i \\ \vdots \\ y_{k-1}^i \end{bmatrix}}_{\mathbf{Y}} \tag{11}$$

where the superscripts "i" and "r" indicate the imaginary and real parts of a complex value, respectively. The solution of (11) gives the partial expansion coefficients, k_i's.

C. Numerical Considerations

The transposed Vandermonde-like matrix in (9), even for moderate order, is notoriously ill-conditioned in the sense that the entries along each row are simple powers of the corresponding frequency values. If the span of the frequencies being considered is large, then the magnitudes of the entries on some of the rows will be much larger than those in rows corresponding to low frequency values. The application of a direct elimination algorithm to solve the Vandermonde-type system in (9) produces unreliable results.

The unequal scale of the rows of $\mathbf{V}$ suggests that there is some artificial ill-conditioning in the problem. The artificial ill-conditioning can be removed. The condition number can be improved by normalizing the maximum frequency to unity. The condition number can still be uncomfortably large, though perhaps good enough for practical purposes, and intolerable for a wide frequency range or high-order approximation. This ill-conditioning is real and will not disappear with any further rescaling. One the other hand, posing the problem in a shifted basis, using the transformation

$$\omega' = 2\frac{(\omega - \omega_{\min})}{(\omega_{\max} - \omega_{\min})} - 1 \tag{12}$$

leads to a better-conditioned problem. Mapping the domain $[\omega_{\min}, \omega_{\max}]$ into $[-1, 1]$ normalizes the domain variable to the center within the numerical range of the computer and minimizes numerical inaccuracies in the solution process.

The minimum number of samples for the interpolation is $k = n$. Since the number of equations is often larger than the number of unknowns, (9) can be transformed into a square matrix using the method of averages [24]. The method of averages is used to obtain a consistent system by adding consecutive equations of the system of equations in (9), into n groups. Due to numerical difficulties, solving the consistent equation obtained from (9) using the direct method, we need an alternative method that does not require a direct elimination method. We seek to transform the problem into a more numerically robust equivalent one, yet still produce the solution. Any matrix can be decomposed in the form $\mathbf{V} = \mathbf{QR}$, where $\mathbf{Q}$ is orthogonal and $\mathbf{R}$ is an upper triangular matrix. For a general matrix, the decomposition is constructed by applying a series of Householder reflectors that zero out all elements in a given column to transform the matrix to a triangular form. Just as in an *LU* factorization, Householder *QR* factorization can be obtained in $(n-1)$ steps. However, unlike the Gaussian elimination process, the Householder *QR* decomposition can always be carried out to completion. Then, the solution of the following triangular system

$$\mathbf{R}X = \mathbf{Q}^T Y \tag{13}$$

is obtained more accurately.

The orthogonal triangularization method is unconditionally stable; there is a no *growth factor*, the growth of the elements in the reduced matrices, to worry about as in Gaussian elimination [25]. For the ill-conditioned problem, the orthogonal

$$\begin{bmatrix} 1 & \omega_0^2 & \omega_0^4 & \cdots & \omega_0^{2\xi} & -\omega_0^2 y_0^r & -\omega_0^4 y_0^r & \cdots & -\omega_0^{2\vartheta} y_0^r \\ 1 & \omega_1^2 & \omega_1^4 & \cdots & \omega_1^{2\xi} & -\omega_1^2 y_1^r & -\omega_1^4 y_1^r & \cdots & -\omega_1^{\vartheta} y_1^r \\ & \vdots & & & & \vdots & & & \\ 1 & \omega_{k-1}^2 & \omega_{k-1}^4 & \cdots & \omega_{k-1}^{2\xi} & -\omega_{k-1}^2 y_{k-1}^r & -\omega_{k-1}^4 y_{k-1}^r & \cdots & -\omega_{k-1}^{2\vartheta} y_{k-1}^r \end{bmatrix} \begin{bmatrix} c_0 \\ c_1 \\ c_2 \\ \vdots \\ c_\xi \\ p_1 \\ p_2 \\ \vdots \\ p_\vartheta \end{bmatrix} = \begin{bmatrix} y_0^r \\ y_1^r \\ \vdots \\ y_{k-1}^r \end{bmatrix} \tag{9}$$

method gives an added measure of reliability. Even if the matrix is not full rank or the system is near singular, the orthogonal factorization still exists. The decomposition of a matrix gives a nonsingular upper triangular matrix whenever the column vectors of $\mathbf{V}$ form a linearly independent sets of vectors. Thus, the triangular system (13) can be solved to high accuracy. The method is comparable with LU factorization in efficiency. It has a computational complexity of $2n^3/3$, and the cost for the triangular system is only $O(n^2)$. The right-hand side of (13) does not need $\mathbf{Q}$ explicitly, the Householder matrices are used to obtain $\mathbf{Q}^T Y$.

The method is also known as the Golub–Householder method because the idea of solving the least-squares problem based on the QR factorization of $\mathbf{V}$ using the Householder transformation was first suggested by G. H. Golub [26]. For a matrix $\mathbf{V} \in \mathbf{R}^{k\times n}$ with $\mathrm{rank}(\mathbf{V}) = n$ and the vector matrix $Y \in \mathbf{R}^k$, the Golub–Householder method computes the least-squares solution $X \in \mathbf{R}^n$ using Householder matrices $\mathbf{H}_1$ through $\mathbf{H}_n$, with the cost of $n^2(k - \frac{n}{3})$. The matrix is decomposed as $\mathbf{V} = \mathbf{H}_1\mathbf{H}_2\cdots\mathbf{H}_{n-1}\mathbf{H}_n\mathbf{R}$ and then the right-hand side is modified as $\mathbf{Q}^T Y = \mathbf{H}_n\mathbf{H}_{n-1}\cdots\mathbf{H}_2\mathbf{H}_1 Y$.

The residue calculation step does not have numerical problems. The system of equations in (11) is well conditioned since the entries of the matrix are of the form $p_j(\omega_i^2 + p_j^2)^{-1}$. In [24], the least-squares solution is obtained using the normal equation method. Since the normal equation method has numerical difficulties, the matrix $\mathbf{M}^T\mathbf{M}$ is frequently ill-conditioned and influenced greatly by round-off errors. Instead, the least-squares solution of (11) is obtained using Householder *QR* orthogonalization.

The approximation problem is solved by building up and solving a linear system of equation. It is obvious that this requires only a small amount of CPU-time, especially since the system is rather small. The total computational complexity of the approximation method is one polynomial factorization, two Householder *QR* transformations, and two backsubstitutions. The algorithm is given in pseudo-code in Algorithm 1 below.

Algorithm 1:

$R\_Approximation(\omega, F, \xi, \vartheta)$

Step 1) Normalize and shift frequency points to map $[\omega_{\min}, \omega_{\max}]$ into $[-1, 1]$ using (12)

Step 2) Construct real matrix of the real part of the function (7):

$\mathbf{V} \in \mathbf{R}^{k\times n}$, $X \in \mathbf{R}^n$, $Y \in R^k$

formulate square matrix using the method of averages:

$\hat{\mathbf{V}} \in \mathbf{R}^{n\times n}$, $\hat{X}, \hat{Y} \in \mathbf{R}^n$

perform Householder *QR* factorization: $\hat{\mathbf{V}} = \mathbf{QR}$

solve: $\mathbf{R}\hat{X} = \mathbf{Q}^T\hat{Y}$

Step 3) If a solution is not acceptable,

select new order of approximation, ξ' and ϑ' and repeat Step 2.

Step 4) Factor denominator and filter the poles,

if the remaining poles are unacceptable go to Step 3.

Step 5) Construct residue matrix (11)

perform Householder QR factorization: $\mathbf{M} = \mathbf{QR}$

solve: $\mathbf{R}X = \mathbf{Q}^T Y$:

Step 6) Return partial fraction expansion

$$H(s) = k_\infty + \sum_{i=1}^{\vartheta'} \frac{k_i}{s + p_i}.$$

V. Integration Method

To avoid an explicit convolution problem, which is computationally expensive in terms of storage and run time, a recursive convolution is applied to obtain the time-domain macromodel of each subnetworks. Recently, a recursive convolution and an indirect numerical integration have been re-established as efficient methods for transient simulation of transmission lines. The integration methods are based on the relationship between the excitation and the response.

The direct relationship between the time and Laplace-domain representation

$$Y(s) = \frac{k_i}{s + p_i} X(s) \leftrightarrow \frac{d}{dt} y(t) + p_i\, y(t) = k_i x(t) \qquad (14)$$

is used to determine the stencils of the multiport subnetworks at each time point using an indirect integration formula. For the step-invariant case, the excitation is assumed to be piecewise constant, $x(t) = c$, where $t_{n-1} \le t \le t_n$ and the differential equation in (14) is solved using the values of the excitation at the current time interval as boundary conditions. Then, the time-domain stamp for the pole-residue model (10) is given as

$$y(t_n) = k_\infty x(t_n) + \sum_{i=1}^{q} \tilde{y}_i(t_n) \qquad (15)$$

where $\tilde{y}_i(t_n) = k_i(1 - e^{-p_i(t_n - t_{n-1})})x(t_{n-1}) + e^{-p_i(t_n - t_{n-1})}\tilde{y}_i(t_{n-1})$.

Equation (15) is implemented as a Norton equivalent circuit consisting of a conductance of constant value, k_∞, and a current source, $-\sum_{i=1}^{q}\tilde{y}_i(t_n)$, that is updated at each time iteration based on the pole-residue pairs and the voltage at a previous one timepoint. Since the number of pole-residue pairs is much smaller than the number of timepoints in the total simulation time, the integration routine is linear in time.

VI. Numerical Results

An interconnect with a V-shaped cross section is characterized using a scattering matrix. The scattering parameters are measured in the frequency range 45 MHz–10 GHz with a *HP8510B* vector network analyzer. The measured scattering parameters of the interconnect are approximated over a frequency range using a rational function. Although

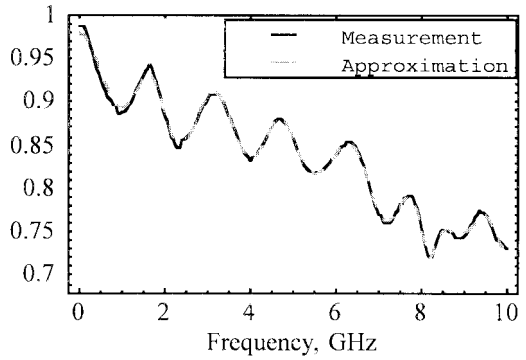

Fig. 2. Magnitude plots of S_{12}, the measured data and the 24th-order rational approximation.

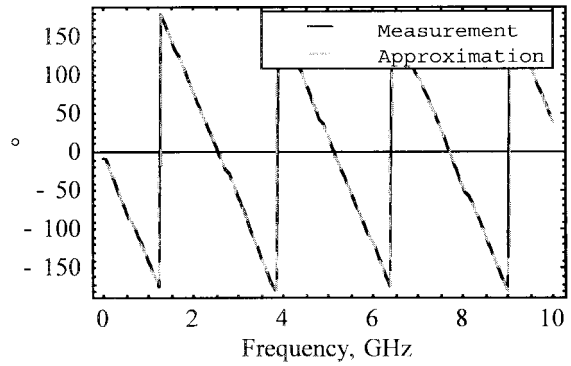

Fig. 3. Phase plots of S_{12}, the measured data and the 24th-order rational approximation.

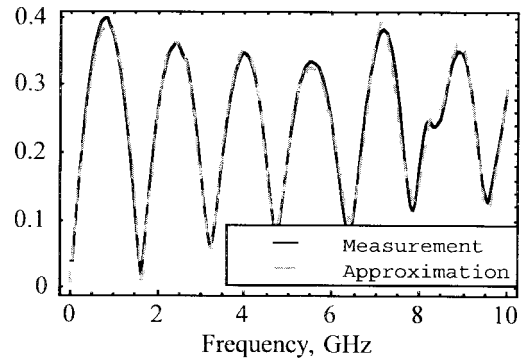

Fig. 4. Magnitude plots of S_{11}, the measured data and the 27th-order rational approximation.

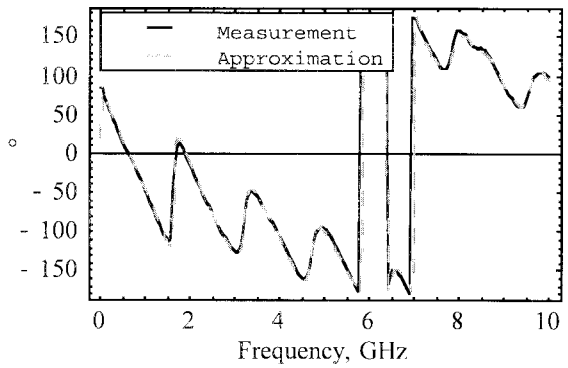

Fig. 5. Phase plots of S_{11}, the measured data and the 27th-order rational approximation.

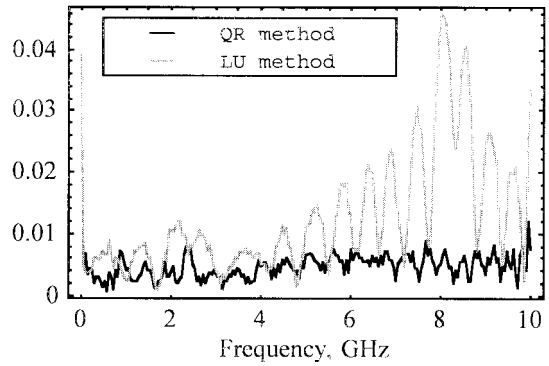

Fig. 6. Magnitude plot of the errors, the 41st-order rational approximation using the method in [24] (gray line), and the proposed method (dark line).

the method is able to generate a stable very high-order rational approximation, a 24th- and a 27th-order rational function is used to approximate S_{12} and S_{11}, respectively. The measured and approximated scattering parameters are shown in Figs. 2–5. The magnitude and phase plots of S_{12} and S_{11} are almost indistinguishable.

A comparison of our method with the method of [24] is shown in Fig. 6. A measure of the quality of the approximations is the normalized numerical difference between the measured data and the rational approximations. The maximum error of the 41st-order approximation with respect to the original S_{11} data is less than 0.8%. The order of approximation is limited to 41, because the direct solution method of [24] becomes numerically unstable when the order approximation is increased beyond 41. The 41st-order of approximation of the proposed method is more accurate as shown in Fig. 6.

A. Example 1: Linear Network

To illustrate the advantage of our method, the network shown in Fig. 7 is analyzed. The network consists of a measured subnetwork characterized by the approximated scattering parameters. First, the measured S-parameters are extrapolated to low frequencies for the dc solution. Then, the scattering parameters are incorporated into the MNA matrix using (2) and dependent sources. The lumped-model subnetwork shown in Fig. 7 is represented as a two-port network in the analysis. A twelfth-order Padé approximation of the admittance matrix of the lumped subnetwork is obtained using Lanczos algorithm [7], [8].

The network is exited by a pulse with rise and fall times of 0.3 ns and pulse magnitude and width of 5 V and 4 ns, respectively. The transient responses of the network at nodes x and y are given in Figs. 8 and 9. The proposed method is compared with the conventional approach in which the exact response is obtained via IFFT. In addition, the application of

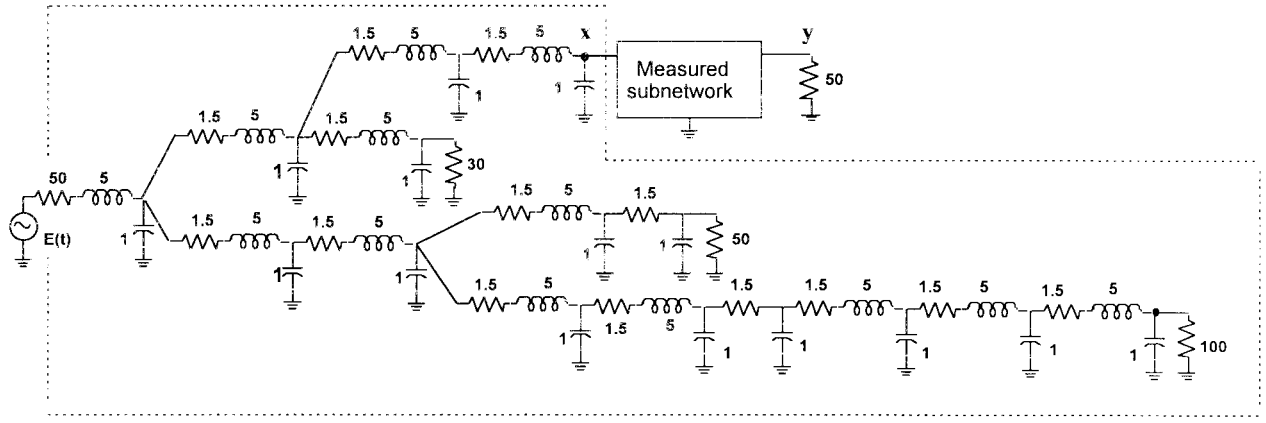

Fig. 7. Example 1, *RLC*-interconnect network with measured component. Padé synthesis and rational approximation are used to generate the pole-residue models of the *RLC* and the measured subnetworks, respectively.

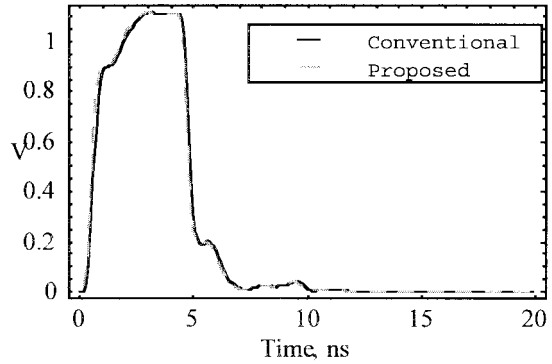

Fig. 8. Example 1, transient response at node x using conventional and the proposed methods.

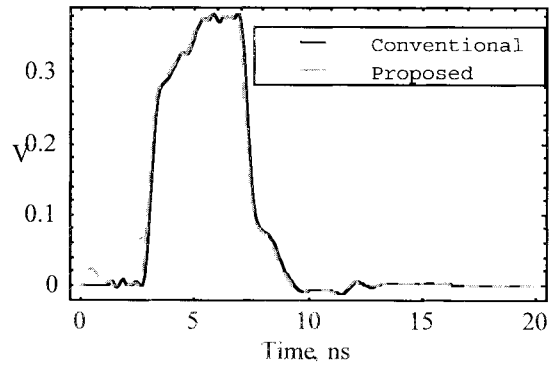

Fig. 9. Example 1, transient response at node y using conventional and the proposed methods.

IFFT for the time-domain solution requires that the scattering parameters be band limited. This is realized using rational function extrapolations. The fact that the two responses are indistinguishable shows that an excellent match has been obtained.

B. Example 2: Nonlinear Network

In Example 2, the proposed method is used to study resistive and diode terminations. The network in Fig. 10 consists

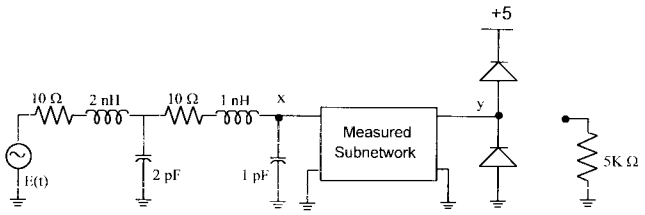

Fig. 10. Example 2, diode-pair terminated network, (the 5-kΩ resistor replaces the diode-pair).

of a measured subnetwork, a diode-pair termination and a resistive termination. For the measured subnetwork, the rational function approximation of the scattering parameters of Example 1 are used. The diode is characterized by $i(t) = I_0(\exp(v(t)/v_T) - 1)$, where $I_0 = 15$ ps and $v_T = 25$ mV.

The network is exited by a pulse with rise and fall times of 0.3 ns and pulse magnitude and width of 5 V and 7 ns, respectively. The network is simulated with the diode-pair termination and with the 5-kΩ resistor replacing the diodes shown in Fig. 10. The transient responses of the diode-pair termination at nodes x and y are compared to those of 5-kΩ resistor termination. At the far-end, node y, the voltage response of the 5-kΩ resistor shows voltage overshoots and undershoots while the diode-pair termination squelch the voltage overshoots as shown in Fig. 11. The voltage waveforms at the near-end, node x, for the two cases are almost identical as shown in Fig. 12. Thus, time-domain analysis of nonlinear network can be performed efficiently using the method.

VII. Conclusion

In this paper, we have presented a robust algorithm for transient simulations of arbitrary interconnect characterized by scattering parameters. The scattering parameters are approximated by rational functions and incorporated directly into the network MNA matrix without converting them into other fundamental parameters or parasitic parameters. Frequency normalization and shift and Householder *QR* orthogonaliza-

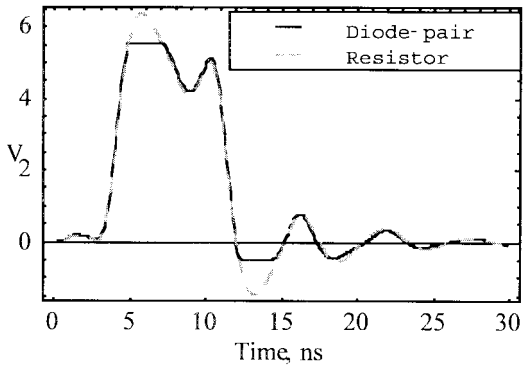

Fig. 11. Example 2, transient response at node y, with diode-pair and resistor terminations.

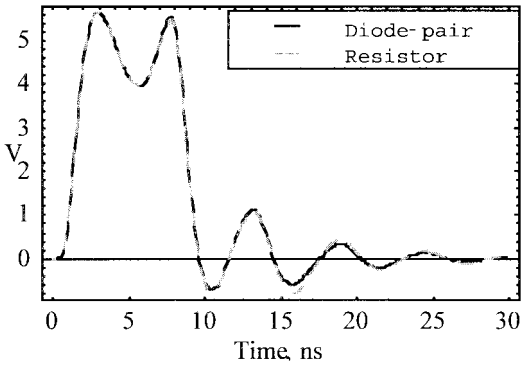

Fig. 12. Example 2, transient response at node x, with diode-pair and resistor terminations.

tion techniques are used to obtain accurate approximations. The analyticity of a scattering matrix is utilized to obtain stable pole-residue pairs using two linear solutions and one polynomial factorization. This leads to a significant reduction in the computational cost compared to that of the costly nonlinear optimization. The necessary numerical considerations in the actual implementation of the algorithm are discussed. The transfer function can be used for time- or frequency-domain analysis of arbitrary networks. Recursive convolution is applied to obtain time-domain macromodels directly from the scattering matrix approximation. Thus, the method avoids numerical transformation and low-pass filtering of sampled data with a large number of frequency points. The validity and accuracy of the method for the transient simulation of linear and nonlinear networks are shown by example.

ACKNOWLEDGMENT

The authors wish to thank Dr. D. Kuznetsov for fruitful discussions on difference approximation that formed the basis of our work presented here, and P. Saylor, University of Illinois, for many helpful suggestions.

REFERENCES

[1] S. B. Goldberg, M. B. Steer, P. D. Franson, and J. S. Kasten, "Experimental electrical characterization of interconnects and discontinuities in high-speed digital systems," *IEEE Trans. Comp., Hybrids, Manufact. Technol.*, vol. 14, Dec. 1991.

[2] L. W. Nagel, "SPICE2: A computer program to simulate semiconductor circuits," Tech. Rep. ERL-M520, Univ. California, Berkeley, May 1975.

[3] W. T. Weeks, A. J. Jininez, G. W. Mahoney, D. Mehta, H. Qassemzadeh, and T. R. Scott, "Algorithms for ASTAP-A network analysis program," *IEEE Trans. Circuit Theory*, vol. CT-20, pp. 628–634, Nov. 1973.

[4] L. Pillage, C. Wolff, and R. Rohrer, "AWEsim: Asymptotic waveform evaluation for timing analysis," in *Proc. 26th Design Automat. Conf.*, 1989.

[5] J. Bracken, V. Raghavan, and R. Rohrer, "Interconnect simulation with asymptotic waveform evaluation (AWE)," *IEEE Trans. Circuit Syst. I*, vol. 39, pp. 869–878, Nov. 1992.

[6] E. Chiprout and M. S. Nakhla, *Asymptotic Waveform Evaluation and Moment Matching for Interconnect Analysis*. Boston, MA: Kluwer, 1994.

[7] ———, "Transient waveform estimation of high-speed MCM networks using complex frequency hopping," in *Proc. Multi-Chip Module Conf. (MCMC)*, Mar. 1993, pp. 134–139.

[8] K. Gallivan, E. Grimme, and P. Van Dooren, "Asymptotic waveform evaluation via Lanczos methods," *Appl. Math. Lett.*, vol. 7, pp. 75–80, 1994.

[9] P. Feldmann and R. W. Freund, "Efficient linear circuit analysis by Padé approximation via the Lanczos process," *IEEE Trans. Computer-Aided Design*, vol. 14, May 1995.

[10] R. Wang and O. Wing, "Analysis of VLSI multiconductor systems by bi-level waveform relaxation," in *Proc. IEEE Int. Conf. CAD*, Oct. 1990, pp. 166–169.

[11] W. T. Beyene, "Bi-level waveform relaxation analysis of package interconnects using scattering parameters," in *Proc. Int. Symp. Microelectron.*, San Francisco, CA, 1992.

[12] J. Schutt-Ainé and R. Mittra, "Scattering parameter transient analysis of transmission lines loaded with nonlinear terminations," *IEEE Trans. Microwave Theory Technol.*, vol. 36, Mar. 1988.

[13] M. Celik and A. C. Cangellaris, "Efficient transient simulation of lossy packaging interconnects using moment-matching techniques," *IEEE Trans. Comp., Hybrids, Manufact. Technol.*, vol. 19, pp. 64–73, Feb. 1996.

[14] R. Sanaie, E. Chiprout, M. S. Nakhla, and Q. J. Zhang, "Integrating subnetwork characterized by measured data into moment-matching simulations," in *Proc. Multi-Chip Module Conf.*, Mar. 1994, pp. 114–119.

[15] R. Sanaie and M. Nakhla, "A fast method for frequency and time domain simulation of high-speed VLSI interconnects," *IEEE Trans. Microwave Theory Tech.*, vol. 42, pp. 2562–2571, Dec. 1994.

[16] C. Ho, A. Ruehli, and P. Brennan, "The modified nodal approach to network analysis," *IEEE Trans. Circuits Syst.*, vol. CAS-22, pp. 504–509, June 1975.

[17] W. T. Beyene and J. E. Schutt-Ainé, "Integrating data obtained from electromagnetic field analysis into frequency- and time-domain circuit simulations," in *Proc. 13th Annu. Rev. Progress Appl. Computat. Electromag.*, Monterey, CA, Mar. 17–21, 1997, pp. 156–163.

[18] E. C. Levy, "Complex curve-fitting," *IRE Trans. Automat. Contr.*, vol. AC-4, pp. 37–44, May 1959.

[19] C. K. Sanathanan and J. Koerner, "Transfer function synthesis as a ratio of two complex polynomials," *IEEE Trans. Automat. Contr.*, vol. 8, pp. 56–58, Jan. 1963.

[20] D. L. Fletcher and C. N. Weygandt, "A digital method of transfer function calculation," *IEEE Trans. Circuit Theory*, vol. CT-18, pp. 185–187, Jan. 1971.

[21] R. J. Bowman and C. C. Brewster, "Determining the zeros and poles of linear circuit networks using function approximation," *IEEE Trans. Computer-Aided Design*, vol. CAD-6, pp. 678–689, July 1987.

[22] C. E. Baumgartner, "On the representation of coupled lossy transmission lines using transfer functions," in *Proc. 9th Annu. Int. Phoenix Conf. Comput. Commun.*, Scottsdale, AZ, Mar. 21–23, 1990.

[23] M. Silveria, I. Elfadel, J. White, M. Chilukuri, and K. Kenneth, "Efficient frequency-domain modeling and circuit simulation of transmission lines," *IEEE Trans. Comp., Hybrids, Manufact. Technol.*, vol. 17, Nov. 1994.

[24] D. Kuznetsov and J. E. Schutt-Ainé "Optimal transient simulation of transmission lines," *IEEE Trans. Circuits Syst. I*, vol. 43, Feb. 1996.

[25] G. W. Stewart, *Introduction to Matrix Computations*. New York: Academic, 1973.

[26] G. Golub, "Numerical methods for solving linear least squares problems," *Numerische Mathematik*, vol. 7, pp. 206–216, 1965.

Wendemagegnehu T. Beyene (S'87–M'88) was born in Addis Ababa, Ethiopia. He received the B.S. and M.S. degrees in electrical engineering from Columbia University, New York, NY, in 1988 and 1991, respectively, and the Ph.D. degree in electrical and computer engineering from the University of Illinois, Urbana-Champaign, in 1997.

From 1988 to 1994, he was with IBM's Microelectronics division, East Fishkill, NY, where he worked on electrical analysis and characterization of advanced electronic packages. In the summer of 1994, he worked on Sneak analysis of electronic hardware and software systems at the Ford Research Laboratory, Dearborn, MI. Presently, he is with Hewlett-Packard EEsof Division, Westlake Village, CA. His professional interests include circuit simulation, field simulation of devices and electromagnetic systems, and signal integrity analysis and efficient simulation of package interconnects at chip, module and board levels.

Dr. Beyene is a member of Eta Kappa Nu, Tau Beta Pi, and SIAM.

José E. Schutt-Ainé (S'86–M'88) received the B.S. degree from the Massachusetts Institute of Technology (MIT), Cambridge, in 1981, and the M.S. and Ph.D. degrees from the University of Illinois, Urbana-Champaign, in 1984 and 1988, respectively.

Following his graduation from MIT he spent two years with Hewlett-Packard Microwave Technology Center, Santa Rosa, CA, where he worked as a Device Application Engineer. While pursuing his graduate studies at the University of Illinois, he held summer positions at GTE Network Systems, Northlake, IL. He is presently serving on the faculty of the Department of Electrical and Computer Engineering, University of Illinois, as an Associate Professor. His interests include microwave theory and measurements, electromagnetics, high-speed digital circuits, solid-state electronics, circuit design, and electronic packaging.